k_r = coefficient of thermal transport by radiation, B.t.u./(hr.) (ft.) (°F.)
k_s = coefficient of thermal transport through stem, B.t.u./(hr.) (ft.) (°F.)
k_{st} = thermal conductivity of steel, B.t.u./(hr.) (ft.) (°F.)
$\dot{q}_c$ = rate of heat transfer by conduction through the fluid, B.t.u. per hour
$\dot{q}_m$ = measured rate of energy addition, B.t.u. per hour
$\dot{q}_p$ = rate of heat transfer through pins, B.t.u. per hour
$\dot{q}_r$ = rate of heat transfer by radiation, B.t.u. per hour
$\dot{q}_s$ = rate of heat transfer through stem, B.t.u. per hour
r_i = inner radius, feet
r_o = outer radius, feet
r_p = radius of pins, feet
t_i = temperature at inner radius, °F.
t_o = temperature at outer radius, °F.
ϵ = emissivity
ϕ ( ) = function of
ϕA = ratio of area of complete sphere to area of sphere minus area intercepted by shaft

LITERATURE CITED

(1) Comings, E. W., Nathan, M. F., *Ind. Eng. Chem.* **39**, 964 (1947).
(2) Eucken, A., *Physik Z.* **14**, 324 (1913).
(3) Golding, B. H., Sage, B. H., *Ind. Eng. Chem.* **43**, 160 (1951).
(4) Hilsenrath, J. and others, "Tables of Thermal Properties of Gases," Natl. Bur. Standards, Circ. **564** (1955).
(5) Hilsenrath, J., Touloukian, Y. S., *Trans. Am. Soc. Mech. Engrs.* **76**, 967 (1954).
(6) Johnston, H. L., Giauque, W. F., *J. Am. Chem. Soc.* **51**, 3194 (1929).
(7) Johnston, H. L., Grilly, E. R., *J. Chem. Phys.* **14**, 233 (1946).
(8) Meyers, C. H., *Bur. Standards J. Research* **9**, 807 (1932).
(9) Opfell, J. B., Schlinger, W. G., Sage, B. H., *Ind. Eng. Chem.* **46**, 189 (1954).
(10) Richter, G. N., Sage, B. H., *Ind. Eng. Chem., Chem. Eng. Data Ser.* **2**, No. 1, 61 (1957).
(11) Todd, G. W., *Proc. Roy. Soc. (London)* **A 83**, 19 (1909).
(12) Winkelmann, A., *Ann. phys.* **156**, 497 (1875).
(13) Wooley, H. W., "Thermodynamic Properties of Gaseous Nitric Oxide," Natl. Bur. Standards, Rept. **2602** (1955).
(14) Yost, D. M., Russell, H., Jr., "Systematic Inorganic Chemistry," Chap. I, Prentice-Hall, New York, 1944.

Received for review November 14, 1957. Accepted June 2, 1958. Work sponsored by Project SQUID which is supported by the Office of Naval Research under Contract N6-ori-105, T. O. III, NR-098-038. Reproduction in full or in part is permitted for any use of the United States Government.

Low Temperature Vapor-Liquid Equilibrium in Light Hydrocarbon Mixtures: Methane-Ethane-Propane System

A. ROY PRICE[1] and RIKI KOBAYASHI
The Rice Institute, Houston, Tex.

While the vapor-liquid equilibrium data for light hydrocarbons are relatively abundant above 50° F., a review of the literature indicates a need for such data at lower temperatures and high pressures. Very few phase equilibria data are available with which to test correlations extending into the low temperature regions. The systems which have been studied heretofore (and their references) are listed below:

System	Source
Methane-ethylene	(*9, 34*)
Methane-ethane	(*3, 14, 25*)
Methane-propane	(*1, 27*)
Methane-n-butane	(*18, 28*)
Ethylene-ethane	(*13, 15*)
Ethylene-propane	(*16, 26*)
Ethylene-propylene	(*16*)
Methane-ethylene-ethane	(*9*)
Ethylene-ethane-acetylene	(*15*)
Natural gases	(*6, 7, 31*)

The purpose of this investigation was to obtain phase equilibria data at low temperatures to supplement the data above and provide a basis for the evaluation of correlations for low temperature K-values. The ternary methane-ethane-propane system was selected because of its basic, yet multicomponent nature. Six temperatures were investigated, extending from 50° down to −200° F. Pressures at 100 and 200 p.s.i. intervals up to the critical states were chosen.

EXPERIMENTAL APPARATUS

The vapor recycle equipment used by Harvey (*10*) was modified for this study. The apparatus can be divided into six functional sections: equilibrium, pressure control, temperature control, charge, sampling, and vacuum systems.

[1]Present address, Humble Oil and Refining Co., Baytown, Tex.

Figure 1 presents the assembly diagram of the experimental apparatus.

The equilibrium cell, C, is submerged in a constant temperature bath contained in a Dewar flask. A Jerguson transparent gage with stainless steel body was used for the cell. Inlet and outlet holes were drilled in the bottom and top, respectively. Thermocouple wells of capillary steel tubing were inserted about an inch from the top and bottom, and a liquid sample tap was drilled near the bottom. Teflon gaskets were used between the glass windows and the metal body, and have been successful down to −250° F. at pressures up to 2000 p.s.i. The windows of the equilibrium cell were centered with respect to the slits in the Dewar flask to permit clear visibility of the cell contents at all times.

Another Jerguson transparent gage, R, was located outside the bath to permit detection of any retrograde condensation of the recycle vapors at room temperature. A totally enclosed magnetic pump, P, provided the recirculation without introducing a source of high pressure leaks. The variable volume cell, V, served as a reservoir of vapor and also as a mercury receptacle used in the regulation of pressure during the charging, equilibration, and liquid sampling periods.

The primary cooling system was similar to that used by Bloomer and others in their study of the methane-ethane system (*3*). The temperature regulation was provided by controlling the rate of evaporation of liquid nitrogen. In this manner, temperature could be regulated to within 0.1° F. of a preassigned value. Calibrated copper-constantan thermocouples placed in the two thermowells and at three locations within the liquid bath indicated the temperature.

The various ternary mixtures studied were synthesized within the equilibrium cell by a trial and error procedure of adding each pure component into the cell. The last traces of heavy hydrocarbons, water, and carbon dioxide were

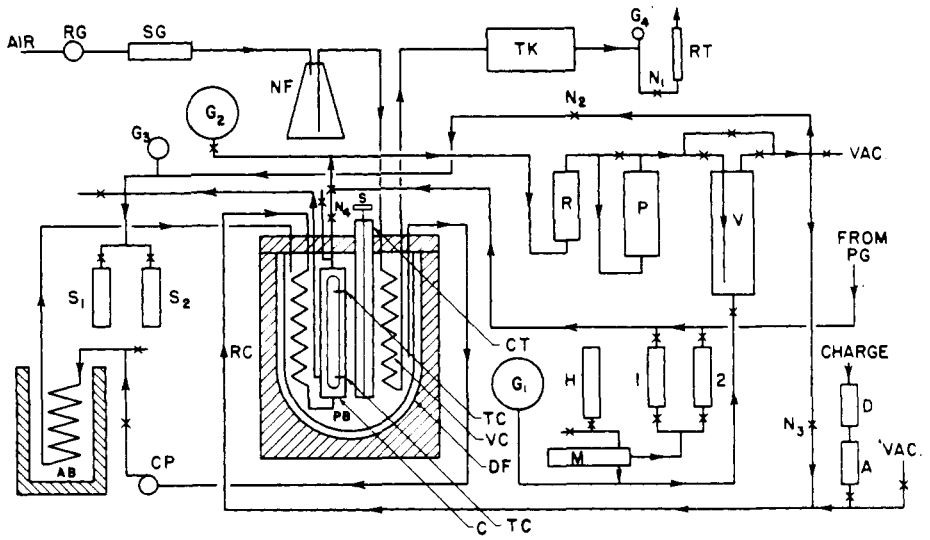

Figure 1. Assembly diagram of experimental apparatus

A.	Ascarite drier
AB.	Alcohol bath
AC.	Auxiliary cooling coil
B_1, B_2, B_3,	Calibrated volumetric bulbs
C.	Visual equilibrium cell
CH.	Charge
CP.	Centrifugal pump
CT.	Copper tube with slits for bath circulation
D.	Drierite drier
D_1, D_2.	Stainless steel drying tubes
DF.	Dewar flask
E.	Equilibrium section
F.	Calibrated glass mixing flask
G_1, G_2, G_3 G_4, G_5.	Pressure gages
H.	Mercury reservoir
M.	Mercury pump
MN.	Manometer
N.	Needle valve
NB.	Liquid nitrogen bath
NF.	Liquid nitrogen flask
P.	Magnetic pump
PB.	Primary bath
PG.	Pressure generator
PV.	Pressure vessel
R.	Visual cell for retrograde condensation
RC.	Recycle coil
RD.	Rupture disk
RG.	Low pressure regulator
RT.	Gas rotameter
S	Air-powered stirrer
S_1, S_2.	Sample containers
SG.	Silica gel driers
TC.	Thermocouple well
TK.	Surge tank
V.	Variable volume cell
Vac.	Vacuum
VC.	Vaporization coil
W.	Water bath
1, 2.	Special charge cylinders
X.	Needle valve
X.	Glass stopcock

removed from the gases by successive contact with activated carbon, Drierite, and Ascarite.

After thermal equilibrium in the cell had been reached, it was found that thermodynamic equilibrium was ensured by circulating the vapors at full recycle rate for 30 minutes and at a reduced recycle rate for approximately 30 more minutes. A recycle coil, *RC*, cooled the recycle vapors to the bath temperature before entering the equilibrium cell. This recycle period was sufficient to ensure that the composition of the vapors in the variable volume cell was identical with the equilibrium vapor in the equilibrium cell. The vapor trapped in the variable volume cell after the liquid sample was taken served as the vapor sample.

The liquid sample was taken through a capillary tube from the side but near the bottom of the equilibrium cell. The capillary tubing outside the bath was wrapped with resistance wire, so that the fluid in the sample lines could be heated during the sample operation. The snug-fitting Nichrome wire was inserted in the line between the sample valve and the equilibrium cell to minimize holdup in the sample line.

MATERIALS

The gases used were obtained from the following sources: methane, Phillips Petroleum Co., Research grade, 99.5%; methane, Tennessee Gas Transmission Co., line gas from selected dehydration station, 99.6%; ethane, Phillips Petroleum Co., Research grade, 99.9%; and propane, Phillips Petroleum Co., Pure grade, 99.0%.

ANALYTICAL METHODS

Two methods were used to determine the composition of the equilibrium phases: infrared spectroscopy and gas-liquid partition chromatography. In general, the infrared analyses were confined to the concentration region in which all components exceeded 10 mole %. Chromatography proved particularly useful in obtaining the analysis in concentration regions where one or more of the components was dilute. Frequent comparisons of the analyses by the two methods were made to check for mutual consistency.

Infrared Analyses. A standard Beckman IR-2 infrared spectrophotometer equipped with a modified 50-cm. gas cell was available for the analyses. The following wave lengths in the infrared region proved to have favorable absorption characteristics and low interference: methane: 7.78 microns; ethane: 9.43 microns; and propane: 12.34 microns. Some interference, however, did occur and it was necessary to develop calibration curves (such as those presented in Figures 2, 3, and 4) from analyses of known synthetic mixtures. Methane did not interfere with the absorption either at the ethane or propane wave lengths; hence the parameters are shown as per cent propane on the ethane plot and per cent ethane on the propane calibration. Serious flattening of the methane curve prevented accurate determination of methane by direct measurement.

To analyze a given gas mixture, absorbance measurements were made on the gas at the ethane and propane wave lengths, and corresponding total pressures. As the compositions of the mixtures were not known, successive ap-

proximations for the propane and then ethane concentrations were made through the use of expanded figures similar to Figures 2, 3, and 4 to establish their concentrations. Because the measurements were made at reduced pressures, Dalton's law was assumed to hold to convert from partial pressures to mole fractions. The concentration of methane was obtained by difference when infrared analyses were made.

Chromatographic Analyses. Gas-liquid partition chromatography (GLPC) was investigated as an alternative analytical method, especially for applications in which the concentration of at least one of the components was low (*23*). At the time of the investigation (spring of 1955) few publications on gas-liquid partition chromatography existed (*5, 11, 12, 20, 21, 24*), none emphasizing high analytical accuracy. Considerable aid in the development of a procedure for accurate analysis by chromatographic means was obtained from the Houston Research Laboratory of Shell Chemical Corp. Of the several liquids tried, kerosine was chosen for the fixed liquid phase. The solid phase selected was crushed, screened Celite C-3 firebrick manufactured by Johns-Manville. Helium was used as the carrier gas because its high thermal conductivity permitted ease of detection with a commercial thermal conductivity cell. The diagram of the chromatographic apparatus is presented in Figure 5.

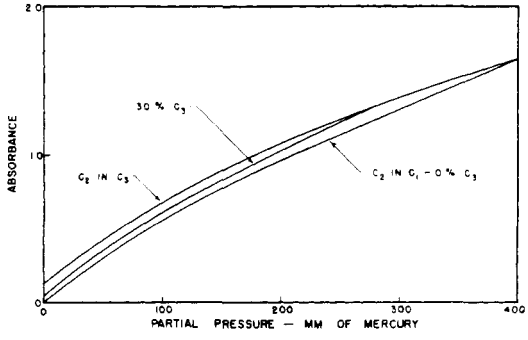

Figure 2. Ethane calibration curve for infrared analysis

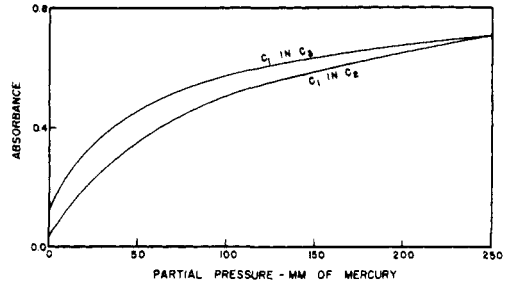

Figure 4. Methane calibration curve for methane analysis (approximate analysis only)

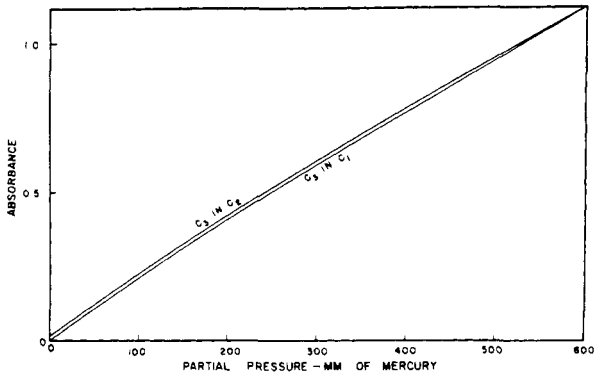

Figure 3. Propane calibration curve for infrared analysis

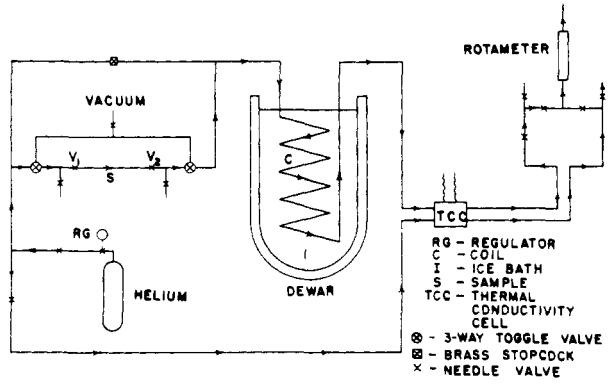

Figure 5. Diagram of chromatographic apparatus

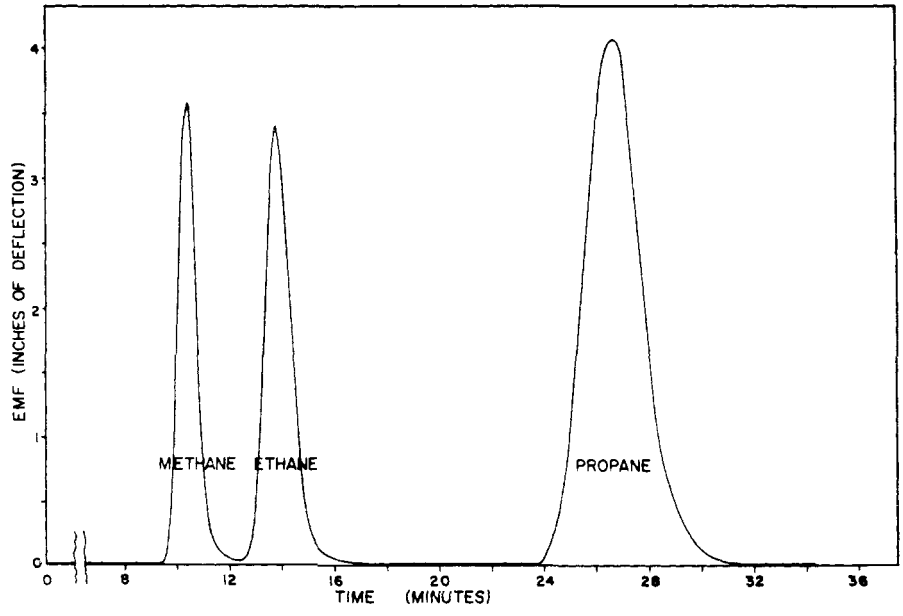

Figure 6. Typical elution curves

The output from the conductivity cell was amplified as desired by means of an attenuated linear direct current amplifier. In this way, the peak areas were adjusted to give the greatest measurable areas by means of a planimeter. The temperature-sensitive portions of the chromatographic apparatus were placed in a constant temperature ice bath. Gas flow rates were adjusted by means of pressure regulators and rotameters. It was imperative that the cell current, zero output base line, gas flow rate, and cell temperature remain constant during analyses. A 2-hour stabilization period was allowed before starting any analysis.

Figure 6 shows a set of elution curves from a typical sample, analyzed as 50–40–10 in mole percentages of methane, ethane, and propane, respectively. The degree of resolution between components depends upon the relative solubilities of the components, the length of the column, and only slightly upon flow rate.

There is a direct relation between the areas under the peaks and the amount of the components in the sample. Because the concentration, y, of the eluted gases in the carrier stream is so low (about 0.5%) the thermal conductivity vs. concentration curves are assumed straight for this concentration range. The e.m.f. from the conductivity cell is in direct proportion to the thermal conductivity of the mixture so the following equation can be written:

$$E = cy \tag{1}$$

where

E = e.m.f. from thermal conductivity cell (expressed in inches of needle deflection)
c = proportionality constant

The area, A_i, under one of the peaks is given by

$$A_i = \int_{t_1}^{t_2} E\,dt \tag{2}$$

where

t = time
t_1 and t_2 = times of initial and final detection of the ith component

Substituting,

$$A_i = \int_{t_1}^{t_2} cy_i\,dt = \int_{t_1}^{t_2} \frac{c}{Q_s}\, y_i\, Q_s\, dt = \frac{c}{Q_s} M_i \tag{3}$$

where

Q_s = flow rate of carrier gas during sample analysis
M_i = moles of component i in sample
(s subscript refers to sample being analyzed)

To eliminate the proportionality constant, Equation 3 is divided by the peak area of a reference sample of the pure component:

$$\frac{A_i}{A_R} = \frac{M_i}{M_R}\,\frac{Q_R}{Q_S} \tag{4}$$

where

M_R = moles of pure component reference sample charged (R subscript refers to reference sample)

M_R may be related to M_s by taking into account differences in compressibility:

$$M_R = M_s \frac{Z_s}{Z_R} \tag{5}$$

where

Z_R, Z_s = compressibility factors for reference and unknown samples respectively
M_s = moles of unknown mixture charged

The volume of sample and the volume of reference sample are equal. The sample for analysis, trapped between valves V_1 and V_2, was vented to the atmosphere prior to charging to facilitate an accurate pressure measurement. The unknown peak area, A_i, is corrected for barometric pressure differences from the reference measurement by including the factor $\frac{P_R}{P_s}$ (P represents barometric pressure). Applying this and Equation 5 to Equation 4:

$$\frac{P_R}{P_s}\,\frac{A_i}{A_R} = \frac{M_i}{M_s}\,\frac{Z_R}{Z_s}\,\frac{Q_R}{Q_s} \tag{6}$$

But $\frac{M_i}{M_s}$ = mole fraction m_i of component i in the unknown sample. Therefore

$$m_i = \frac{A_i}{A_R}\,\frac{Q_s}{Q_R}\,\frac{Z_s}{Z_R}\,\frac{P_R}{P_s} \tag{7}$$

Equation 7 was used to calculate the composition of gas samples from measurements of unknown peak area, reference peak area, and the three correction factors (flow rate, compressibility factor, and barometric pressure). These correction factors were usually small, with a maximum of about 1% for the latter two and 10% for the first. The flow rate correction was determined by an indirect method because the rotameter was too insensitive to changes in flow. Because the initial detection time for a component is inversely proportional to flow rate, the ratio $\frac{t_R}{t_s}$ was substituted for $\frac{Q_s}{Q_R}$

where

t_R, t_s = initial detection times for component in reference measurement and unknown sample, respectively

The two compressibilities, Z_s and Z_R, did not differ greatly; therefore an approximate method was used to estimate Z_s. A rough analysis of the mixture was calculated by taking the area ratio A_i/A_R as mole fraction, m_i, for each component, with proper correction to have $\sum_{i=1}^{n} m_i = 1.0$. Then a molal average compressibility factor was calculated for the sample–i.e.

$$Z_s = \sum_{i=1}^{n} m_i Z_i \tag{8}$$

Compressibility factors were obtained from Silberberg and others (*29*).

The reference areas were checked periodically, but no significant variation was noted. The corresponding areas

Table I. Accuracy Evaluation of Chromatographic Method

	By Synthetic Mixtures, Mole Fraction			By Mass Spectrometer, Mole Fraction		
Component	GLPC	True comp.	% rel. devn.	GLPC	Mass spec.	% rel. devn.
Methane	0.801	0.7994	0.3	0.884	0.882	0.2
Ethane	0.147	0.1498	−1.9	0.0949	0.097	−2.2
Propane	0.0519	0.0508	2.2	0.0212	0.021	1.0
Methane	0.0486	0.0483	0.6	0.441	0.435	1.4
Ethane	0.193	0.1955	−1.3	0.248	0.255	−2.7
Propane	0.758	0.7562	0.2	0.311	0.309	0.7
Methane	0.745	0.7441	0.1	0.424	0.431	−1.6
Ethane	0.231	0.2314	−0.2	0.150	0.153	−2.0
Propane	0.0248	0.0245	1.2	0.426	0.417	2.2
Methane	0.490	0.4905	−0.1	0.801	0.794	0.9
Ethane	0.0112	0.0111	0.9	0.143	0.147	−2.7
Propane	0.498	0.4983	−0.6	0.0559	0.058	−3.6
Methane				0.441	0.436	1.1
Ethane				0.366	0.371	−1.3
Propane				0.193	0.192	0.5

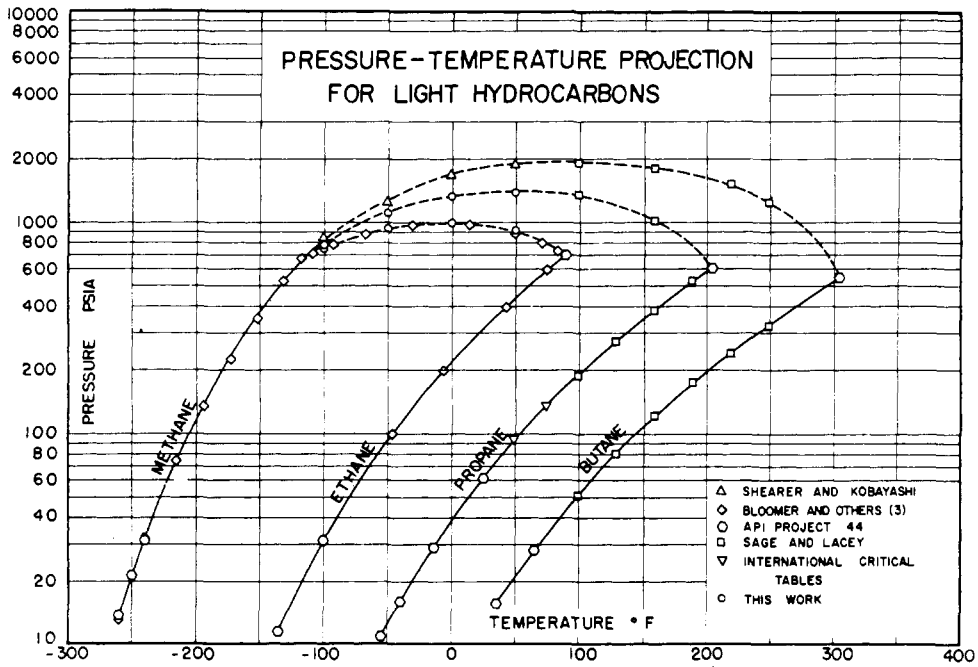

Figure 7. Pressure-temperature projection for light hydrocarbons

and initial detection time at 30.000 inches of mercury barometric pressure were

Component	Initial Detection Time, Minutes	Reference Peak Area, Sq. Cm.
CH_4	9.40	42.9
C_2H_6	12.70	65.7
C_3H_8	24.07	85.1

Peak areas were measured by planimeter to a relative accuracy of 1%. Other indications of area (such as peak height, and peak height times width of elution curve at one half peak height) were investigated, but the accuracy was not satisfactory.

The method was evaluated by analyzing known mixtures and having spot checks made by mass spectrometer. Four synthetic mixtures were prepared in the manner described under infrared analyses and analyzed by gas-liquid partition chromatography. In addition, five samples taken during equilibrium measurements were analyzed chromatographically and checked by mass spectrometer analysis. The results appear in Table I.

In many cases, both infrared and chromatographic analyses were made on the equilibrium samples. Agreement was

(*Text continued on page 49*)

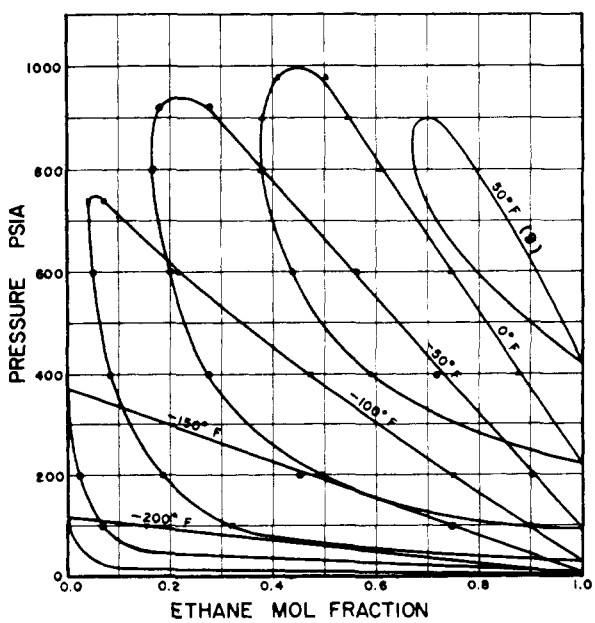

Figure 8. Pressure-composition diagram for methane-ethane system

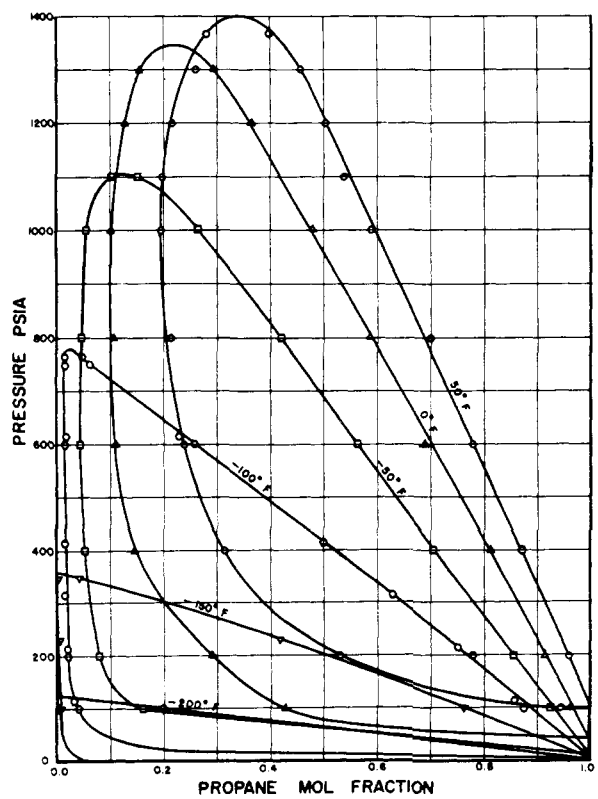

Figure 9. Pressure-composition diagram for methane-propane system

Table II. Results for Binary and Ternary Systems

Temp., °F.	Press. P.S.I.A.	Liquid Composition			Vapor Composition			K-Values					
								CH_4		C_2H_6		C_3H_8	
		CH_4	C_2H_6	C_3H_8	CH_4	C_2H_6	C_3H_8	Exptl.	Smoothed	Exptl.	Smoothed	Exptl.	Smoothed
50	100	0.0028[a]		0.998	0.057		0.943	20.5[a]	20.5			0.945	0.945
50	100	0.0022[a]	0.0080	0.9897	0.0452	0.0280	0.9268	20.4[a]	20.4	3.50	3.27	0.936	0.947
50	100		0.0236	0.9764		0.0720	0.9280			3.05		0.951	
50	200	0.044[a]		0.960	0.471		0.529	10.7[a]	10.3			0.551	0.540
50	200	0.044[a]		0.962	0.471		0.529	10.7[a]				0.550	
50	200	0.0396[a]	0.0655	0.8966	0.412	0.112	0.476	10.4[a]	10.2	1.86	1.80	0.531	0.542
50	200	0.0270[a]	0.160	0.811	0.275	0.284	0.441	10.2[a]	10.1	1.77	1.78	0.543	0.545
50	200	0.0128[a]	0.264	0.7193	0.127	0.476	0.397	9.95	9.95	1.80	1.77	0.552	0.551
50	200		0.357	0.643		0.612	0.388			1.72	1.75	0.603	0.587
50	400	0.128		0.872	0.685		0.315	5.35	5.55			0.361	0.350
50	400	0.110	0.175	0.715	0.557	0.193	0.250	5.06	5.12	1.10	1.07	0.350	0.357
50	400	0.0697	0.500	0.4303	0.306	0.535	0.159	4.39	4.42	1.07	1.07	0.369	0.374
50	400	0.0620	0.553	0.385	0.282	0.570	0.148	4.54	4.33	1.03	1.07	0.348	0.378
50	400	0.0302	0.7578	0.212	0.115	0.7989	0.0861	3.81	3.94	1.05	1.07	0.406	0.398
50	400		0.9066	0.0934		0.9616	0.0384			1.06		0.411	
50	400		0.9108	0.0892		0.9606	0.0394			1.05	1.06	0.442	0.424
50	600	0.216		0.784	0.762		0.238	3.53	3.46			0.304	0.304
50	600	0.214	0.151	0.635	0.663	0.133	0.204	3.10	3.26	0.880	0.860	0.321	0.316
50	600	0.204	0.178	0.618	0.654	0.150	0.196	3.20	3.23	0.843	0.860	0.317	0.320
50	600	0.178	0.376	0.446	0.521	0.332	0.147	2.93	2.95	0.883	0.860	0.330	0.343
50	600	0.174	0.457	0.369	0.487	0.382	0.131	2.80	2.88	0.836	0.860	0.355	0.352
50	600	0.137	0.647	0.216	0.371	0.5501	0.0789	2.71	2.69	0.849	0.860	0.365	0.374
50	600	0.113	0.768	0.119	0.286	0.6668	0.0472	2.53	2.57	0.868	0.860	0.397	0.390
50	600[b]	0.083	0.917		0.210	0.790		2.53	2.43	0.861	0.860		
50	800	0.300		0.700	0.788		0.212	2.63	2.63			0.303	0.303
50	800	0.286	0.121	0.593	0.7224	0.0906	0.187	2.53	2.51	0.749	0.748	0.315	0.312
50	800	0.268	0.359	0.373	0.588	0.282	0.130	2.19	2.18	0.786	0.780	0.348	0.350
50	800	0.255	0.454	0.291	0.534	0.357	0.109	2.10	2.07	0.787	0.790	0.374	0.373
50	800	0.237	0.566	0.197	0.4632	0.455	0.0818	1.95	1.91	0.803	0.803	0.415	0.415
50	800[b]	0.207	0.793		0.325	0.675		1.58	1.58	0.852	0.852		
50	1000	0.413		0.587	0.805		0.195	1.95	1.95			0.332	0.332
50	1000	0.389	0.169	0.442	0.707	0.126	0.167	1.82	1.82	0.745	0.732	0.378	0.379
50	1000	0.385	0.225	0.390	0.680	0.164	0.156	1.76	1.76	0.729	0.732	0.400	0.397
50	1000	0.373	0.357	0.270	0.600	0.268	0.132	1.61	1.61	0.751	0.745	0.442	0.442
50	1000	0.349	0.505	0.146	0.4826	0.431	0.0864	1.38	1.38	0.853	0.855	0.591	0.596
50	1000	0.3755	0.5241	0.1004	0.4345	0.490	0.0755	1.16	1.16	0.933	0.9400	0.751	0.776
50	1100	0.451		0.549	0.803		0.197	1.78	1.77			0.359	0.365
50	1100	0.4365	0.0409	0.5226	0.7746	0.0306	0.1948	1.77	1.77	0.748	0.748	0.373	0.370
50	1100	0.430	0.110	0.460	0.7341	0.0849	0.181	1.71	1.71	0.771	0.749	0.394	0.394
50	1100	0.438	0.192	0.370	0.692	0.143	0.165	1.58	1.58	0.744	0.750	0.446	0.445
50	1100	0.438	0.223	0.339	0.665	0.173	0.162	1.52	1.52	0.776	0.773	0.478	0.478
50	1100	0.435	0.259	0.306	0.630	0.209	0.161	1.45	1.42	0.807	0.815	0.526	0.527
50	1100	0.440	0.376	0.184	0.504	0.351	0.145	1.15	1.12	0.934	0.938	0.788	0.830
50	1200	0.498		0.502	0.784		0.216	1.57	1.56			0.430	0.432
50	1200	0.4997	0.0375	0.4628	0.7558	0.0302	0.214	1.51	1.53	0.806	0.800	0.462	0.458
50	1200	0.504	0.176	0.320	0.673	0.143	0.184	1.34	1.34	0.813	0.813	0.575	0.597
50	1200	0.508	0.243	0.249	0.584	0.219	0.197	1.15	1.15	0.901	0.901	0.791	0.810
0	100	0.0358		0.9642	0.573		0.427	15.9	15.9			0.445	0.412
0	100	0.0335	0.0174	0.9491	0.5589	0.0336	0.4075	16.7	15.8	1.93	1.95	0.430	0.412
0	100	0.0279	0.1284	0.8437	0.400	0.246	0.354	14.3	15.6	1.92	1.95	0.420	0.418
0	100	0.0210	0.166	0.813	0.325	0.349	0.326	15.5	15.4	2.10	1.95	0.401	0.421
0	100	0.0107	0.272	0.7173	0.159	0.534	0.307	14.9	14.8	1.96	1.95	0.428	0.437
0	100		0.373	0.627		0.692	0.308			1.85		0.491	
0	200	0.0904		0.9096	0.768		0.232[c]	8.47	8.47			0.256	0.247
0	200	0.0917	0.0127	0.8956	0.7717	0.0133	0.215	8.43		1.05		0.240	
0	200	0.0702	0.250	0.6798	0.560	0.270	0.170	7.98	8.04	1.08	1.07	0.250	0.256
0	200	0.0457	0.4843	0.470	0.359	0.519	0.122	7.85	7.51	1.07	1.07	0.260	0.264
0	200	0.0127	0.8133	0.174	0.0778	0.8746	0.0476	6.12	6.33	1.08	1.07	0.274	0.278
0	200		0.9013	0.0987		0.9717	0.0283			1.08	1.08	0.287	0.283
0	400	0.199		0.801	0.862		0.138	4.33	4.33			0.172	0.168
0	400	0.159	0.347	0.494	0.6985	0.217	0.0845	4.39	4.17	0.626	0.626	0.171	0.173
0	400	0.1557	0.5293	0.315	0.6003	0.343	0.0567	3.86	3.94	0.648	0.648	0.180	0.181
0	400	0.1364	0.7243	0.1393	0.4869	0.4852	0.0279	3.57	3.63	0.670	0.662	0.200	0.198
0	400[b]	0.123	0.877		0.410	0.590		3.33	3.29	0.673	0.680		
0	600	0.311		0.689	0.891		0.109	2.86	2.86			0.158	0.158
0	600	0.293	0.266	0.441	0.781	0.1377	0.0813	2.67	2.70	0.518	0.518	0.185	0.171
0	600	0.288	0.343	0.369	0.7514	0.184	0.0646	2.61	2.64	0.537	0.527	0.175	0.184
0	600	0.272	0.481	0.247	0.6896	0.260	0.0504	2.54	2.50	0.540	0.549	0.204	0.202
0	600	0.271	0.6204	0.1086	0.6138	0.361	0.0252	2.28	2.32	0.582	0.575	0.232	0.240
0	600[b]	0.256	0.744		0.561	0.439		2.18	2.15	0.591	0.596		
0	800	0.415		0.585	0.899		0.101	2.16	2.16			0.173	0.173
0	800	0.391	0.188	0.421	0.8239	0.0939	0.0822	2.11	2.13	0.499	0.498	0.195	0.191
0	800	0.378	0.354	0.268	0.7727	0.1702	0.0517	2.05	2.03	0.481	0.520	0.213	0.210
0	800	0.380	0.418	0.202	0.7318	0.224	0.0442	1.93	1.97	0.536	0.540	0.219	0.220

Table II. (*Continued*)

Temp., °F.	Press. P.S.I.A.	Liquid Composition			Vapor Composition			*K*-Values					
								CH_4		C_2H_6		C_3H_8	
		CH_4	C_2H_6	C_3H_8	CH_4	C_2H_6	C_3H_8	Exptl.	Smoothed	Exptl.	Smoothed	Exptl.	Smoothed
0	800[b]	0.380	0.5142	0.1058	0.6795	0.296	0.0245	1.80	1.81	0.576	0.576	0.232	0.233
0	800[b]	0.390	0.610		0.619	0.381		1.59	1.58	0.621	0.621		
0	1000	0.522		0.478	0.895		0.105	1.71	1.71			0.220	0.220
0	1000	0.515	0.0780	0.407	0.8623	0.0443	0.0934	1.68	1.68	0.568	0.548	0.230	0.235
0	1000	0.512	0.187	0.301	0.8174	0.1027	0.0799	1.60	1.60	0.549	0.562	0.266	0.266
0	1000	0.514	0.239	0.247	0.791	0.140	0.0690	1.54	1.54	0.586	0.583	0.280	0.288
0	1000	0.5161	0.3378	0.1461	0.7234	0.226	0.0506	1.40	1.40	0.669	0.6430	0.346	0.355
0	1000	0.5258	0.4467	0.0275	0.6357	0.349	0.0153	1.21	1.15	0.781	0.840	0.554	0.618
0	1000[c]	0.522	0.478		0.569	0.431		1.09	1.09	0.901	0.901		
0	1100	0.582		0.418	0.888		0.112	1.53	1.53			0.268	0.268
0	1100	0.5759	0.0581	0.366	0.8619	0.0341	0.104	1.50	1.50	0.587	0.585	0.284	0.284
0	1100	0.585	0.107	0.308	0.8377	0.0635	0.0988	1.43	1.46	0.593	0.585	0.321	0.307
0	1100	0.584	0.157	0.259	0.8237	0.0928	0.0835	1.41	1.41	0.591	0.602	0.322	0.332
0	1100	0.587	0.192	0.221	0.7947	0.1231	0.0822	1.35	1.35	0.641	0.630	0.372	0.364
0	1100	0.582	0.228	0.190	0.7707	0.154	0.0753	1.32	1.28	0.675	0.666	0.396	0.410
0	1100	0.5917	0.2483	0.1600	0.7545	0.1758	0.0697	1.275	1.23	0.708	0.712	0.436	0.460
0	1100	0.6043	0.259	0.1367	0.7484	0.1855	0.0661	1.24	1.19	0.716	0.770	0.484	0.525
0	1100	0.604	0.273	0.123	0.7142	0.2177	0.0681	1.18	1.10	0.797	0.920	0.554	0.710
0	1200	0.637		0.363	0.873		0.127	1.37	1.37			0.350	0.350
0	1200	0.6456	0.0874	0.267	0.8218	0.0625	0.1157	1.27	1.27	0.716	0.710	0.433	0.433
0	1200	0.653	0.106	0.241	0.8158	0.0751	0.1091	1.25	1.23	0.708	0.720	0.453	0.471
0	1200	0.650	0.118	0.232	0.795	0.089	0.116	1.22	1.20	0.754	0.740	0.500	0.507
0	1200	0.693	0.161	0.146	0.721	0.144	0.135	1.04	1.00	0.894	1.00	0.925	1.00
0	1300	0.708		0.292	0.845		0.155	1.19	1.19			0.531	0.531
0	1300	0.7103	0.0297	0.260	0.8294	0.0246	0.146	1.17	1.17	0.828	0.828	0.561	0.560
0	1300	0.7315	0.0345	0.234	0.8086	0.0322	0.1592	1.11	1.11	0.933	0.960	0.681	0.630
0	1300	0.7364	0.0396	0.224	0.7978	0.0384	0.1638	1.08	1.00	0.970	1.00	0.731	1.00
−50	100	0.0769		0.9231	0.840		0.160	10.9	11.5			0.173	0.160
−50	100	0.0614	0.1718	0.7668	0.7195	0.1628	0.1177	11.7	11.3	0.947	0.950	0.153	0.160
−50	100	0.0486	0.302	0.6494	0.605	0.292	0.103	12.4	11.2	0.967	0.950	0.159	0.160
−50	100	0.0479	0.399	0.5531	0.5287	0.380	0.0913	11.0	11.1	0.952	0.950	0.165	0.160
−50	100	0.0467	0.448	0.5053	0.4952	0.425	0.0798	10.6	10.9	0.949	0.950	0.158	0.160
−50	100	0.0261	0.7259	0.248	0.280	0.682	0.0380	10.7	10.8	0.939	0.950	0.153	0.160
−50	100[b]	0.006	0.994		0.066	0.934		11.0	10.7	0.940	0.950		
−50	200	0.146		0.854	0.9216		0.0784	6.31	6.50			0.0918	0.0920
−50	200	0.125	0.268	0.607	0.804	0.140	0.0560	6.43	6.19	0.522	0.530	0.0922	0.0920
−50	200	0.125	0.368	0.507	0.7478	0.206	0.0462	5.98	6.00	0.560	0.531	0.0911	0.0922
−50	200	0.119	0.627	0.254	0.6383	0.333	0.0287	5.35	5.60	0.531	0.534	0.115	0.115
−50	200	0.0968	0.9032		0.505	0.495		5.22	5.00	0.548	0.540		
−50	400	0.296		0.704	0.9493		0.0507	3.20	3.20			0.0735	0.0710
−50	400	0.292	0.126	0.582	0.920	0.0383	0.0417	3.15	3.18	0.304	0.304	0.0717	0.0710
−50	400	0.271	0.289	0.440	0.8791	0.0907	0.0302	3.24	3.11	0.314	0.313	0.0687	0.0710
−50	400	0.274	0.448	0.278	0.8245	0.154	0.0215	3.02	2.97	0.344	0.331	0.0773	0.0750
−50	400	0.270	0.512	0.218	0.8084	0.1742	0.0174	2.99	2.91	0.340	0.340	0.0798	0.0815
−50	400	0.277	0.523	0.200	0.7986	0.1880	0.0134	2.88	2.88	0.359	0.343	0.0805	0.0840
−50	400	0.278	0.571	0.151	0.7901	0.194	0.0159	2.74	2.83	0.340	0.352	0.105	0.0950
−50	400	0.282	0.718		0.724	0.276		2.57	2.61	0.384	0.385		
−50	600	0.438		0.562	0.9585		0.0415	2.19	2.19			0.0739	0.0739
−50	600	0.440	0.145	0.415	0.9179	0.0485	0.0336	2.06	2.11	0.334	0.310	0.0809	0.0795
−50	600	0.424	0.150	0.426	0.919	0.0446	0.0364	2.17	2.11	0.298	0.310	0.0855	0.0800
−50	600	0.443	0.243	0.314	0.8952	0.0790	0.0258	2.02	2.04	0.325	0.317	0.0822	0.0840
−50	600	0.441	0.366	0.193	0.8637	0.119	0.0173	1.96	1.96	0.327	0.330	0.0896	0.0896
−50	600	0.438	0.562		0.800	0.200		1.83	1.83	0.356	0.356		
−50	800	0.581		0.419	0.959		0.0410	1.65	1.65			0.0978	0.0978
−50	800	0.598	0.109	0.293	0.9275	0.362	0.0363	1.55	1.55	0.332	0.322	0.124	0.120
−50	800	0.611	0.249	0.140	0.8901	0.0886	0.0213	1.46	1.44	0.356	0.356	0.152	0.157
−50	800	0.622	0.378		0.832	0.168		1.34	1.34	0.445	0.445		
−50	1000	0.736		0.264	0.9458		0.0542	1.29	1.29			0.205	0.205
−50	1000	0.7609	0.0651	0.174	0.9216	0.0331	0.0453	1.21	1.25	0.509	0.510	0.260	0.275
−50	1000	0.7662	0.0892	0.1446	0.9026	0.0504	0.0470	1.18	1.22	0.565	0.544	0.325	0.320
−50	1000	0.7749	0.1261	0.0990	0.8838	0.0758	0.0404	1.14	1.13	0.609	0.635	0.408	0.452
−50	1000	0.7837	0.1491	0.0672	0.8631	0.1001	0.0368	1.10	1.10	0.671	0.800	0.547	0.650
−50	1000	0.8332	0.1318	0.0350	0.8363	0.1288	0.0349	1.00	1.00	0.977	0.977	0.997	0.995
−100	100	0.125		0.875	0.9591		0.0409	7.67	7.90			0.0468	0.0452
−100	100	0.118	0.144	0.738	0.9186	0.0472	0.0342	7.78	7.78	0.328	0.327	0.0463	0.0452
−100	100	0.110	0.320	0.570	0.8651	0.110	0.0249	7.77	7.60	0.344	0.335	0.0437	0.0453
−100	100	0.110	0.580	0.310	0.7916	0.194	0.0144	7.20	7.26	0.334	0.345	0.0464	0.0456
−100	100	0.101	0.899		0.680	0.320		6.73	6.70	0.356	0.356		
−100	200	0.222		0.778	0.9792		0.0208	4.41	4.40			0.0268	0.0261
−100	200	0.235	0.121	0.644	0.9615	0.0228	0.0157	4.09	4.23	0.188	0.187	0.0254	0.0261
−100	200	0.232	0.435	0.333	0.9070	0.0840	0.00897	3.91	3.81	0.193	0.201	0.0269	0.0261
−100	200	0.236	0.483	0.281	0.8926	0.0983	0.00909	3.78	3.73	0.204	0.205	0.0324	0.0263
−100	200	0.250	0.750		0.814	0.186		3.26	3.21	0.248	0.249		
−100	400	0.477		0.523	0.9855		0.0145[c]	2.06	2.06			0.0277	0.0270
−100	400	0.492	0.175	0.333	0.963	0.0266	0.0104	1.96	1.97	0.152	0.149	0.0312	0.0291

Table II. (*Continued*)

Temp., °F.	Press. P.S.I.A.	Liquid Composition			Vapor Composition			*K*-Values					
								CH_4		C_2H_6		C_3H_8	
		CH_4	C_2H_6	C_3H_8	CH_4	C_2H_6	C_3H_8	Exptl.	Smoothed	Exptl.	Smoothed	Exptl.	Smoothed
−100	400	0.496	0.242	0.262	0.9562	0.0364	0.00741	1.93	1.92	0.150	0.154	0.0283	0.0313
−100	400	0.504	0.308	0.188	0.9446	0.0486	0.00685	1.88	1.86	0.158	0.156	0.0364	0.0362
−100	400	0.5191	0.386	0.0949	0.9321	0.0630	0.00486	1.80	1.80	0.163	0.164	0.0512	0.0481
−100	400	0.528	0.472		0.9165	0.0835		1.72	1.67	0.177	0.178		
−100	600	0.744		0.256	0.9852		0.0148	1.32	1.32			0.0556	0.0540
−100	600	0.745	0.0520	0.203	0.9775	0.0119	0.0106	1.31	1.30	0.229	0.229	0.0522	0.0540
−100	600	0.7647	0.1612	0.0741	0.9583	0.0366	0.00512	1.25	1.25	0.227	0.232	0.0691	0.0660
−100	600	0.784	0.216		0.9498	0.0502		1.21	1.21	0.232	0.237		
−150	100	0.238		0.762	0.9932		0.0068	4.17	4.17			0.0089	0.0080
−150	100	0.242	0.258	0.500	0.9686	0.0282	0.0032	4.00	4.00	0.109	0.110	0.0064	0.0080
−150	100	0.240	0.275	0.485	0.9653	0.0308	0.0039	4.02	3.96	0.112	0.109	0.0080	0.0080
−150	100	0.249	0.446	0.305	0.9538	0.0433	0.0030	3.68	3.82	0.0970	0.103	0.0098	0.0097
−150	100	0.252	0.6762	0.0718	0.9299	0.0682	0.0019	3.67	3.68	0.102	0.0940	0.0265	0.0252
−150	100	0.251	0.749		0.9312	0.0688		3.71	3.61	0.0918	0.0920		
−150	200	0.502		0.498	0.9955		0.0045	1.98	2.01			0.0090	0.0091
−150	200	0.514	0.208	0.278	0.9806	0.0167	0.0027	1.91	1.92	0.0805	0.0860	0.0097	0.0097
−150	200	0.528	0.319	0.153	0.9742	0.0234	0.0024	1.84	1.83	0.0734	0.0745	0.0157	0.0155
−150	200	0.5532	0.400	0.0468	0.969	0.0294	0.0016	1.75	1.76	0.0735	0.0710	0.0342	0.0370
−150	200	0.561	0.439		0.970	0.030		1.73	1.73	0.0683	0.0702		
−200	100	0.802		0.198	0.9993		0.0007[d]	1.24	1.24			0.0035	0.0035
−200	100	0.8075	0.0735	0.119	0.9962	0.0021	0.0007[d]	1.23	1.23	0.0286	0.0337	0.0059	0.0060
−200	100	0.8187	0.124	0.0573	0.9961	0.0029	0.0007[d]	1.22	1.22	0.0234	0.0285	0.012	0.0155
−200	100	0.833	0.167		0.9965	0.0035		1.20	1.21	0.0210	0.0245		

[a] Calculated by Henry's law.
[b] Bloomer and others (*3*).
[c] Interpolated.
[d] Estimated.

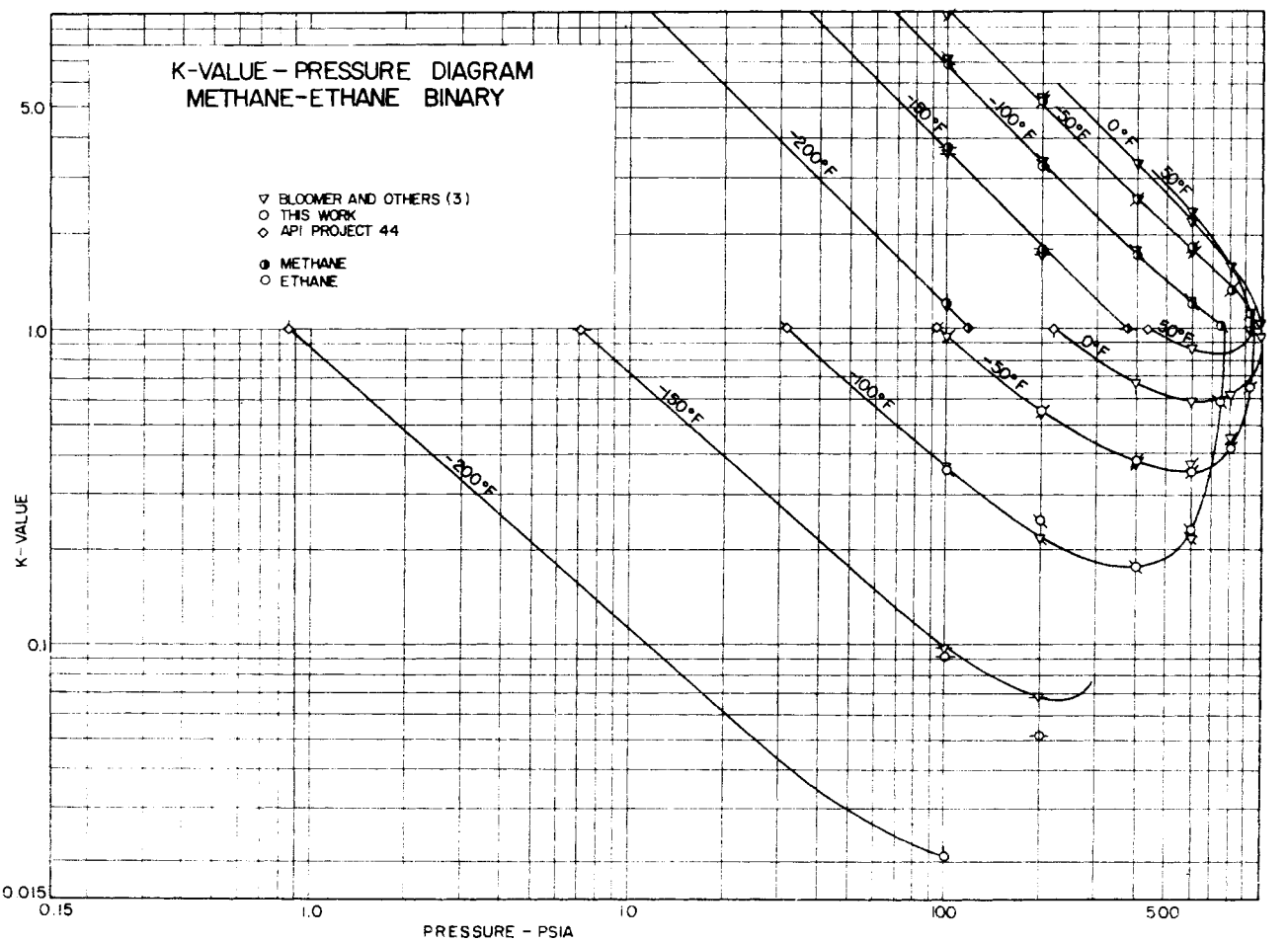

Figure 10. *K*-value-pressure diagram for methane-ethane system

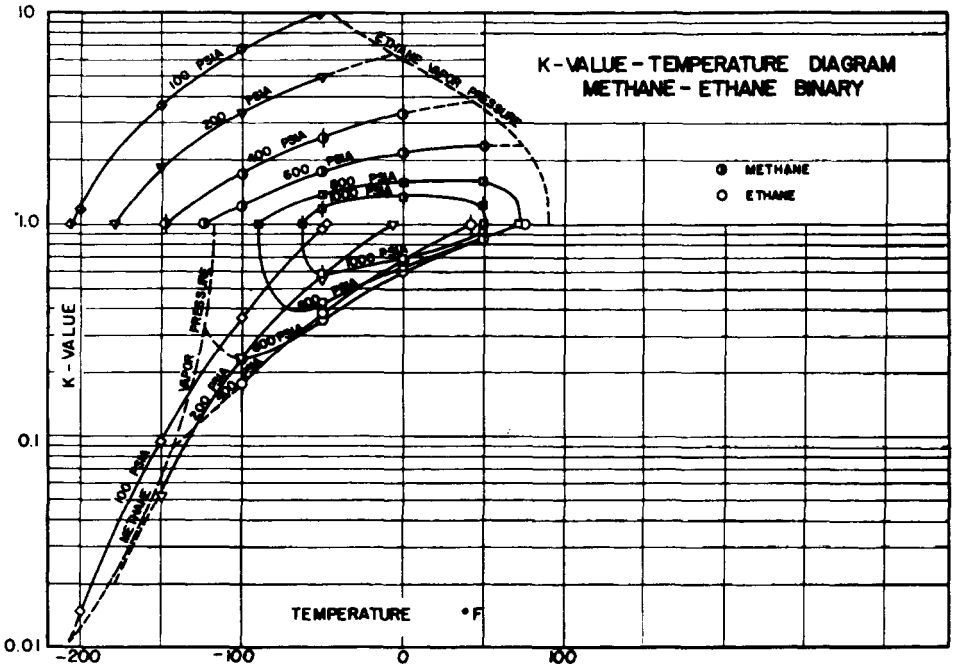

Figure 11. *K*-value–temperature diagram for methane-ethane system

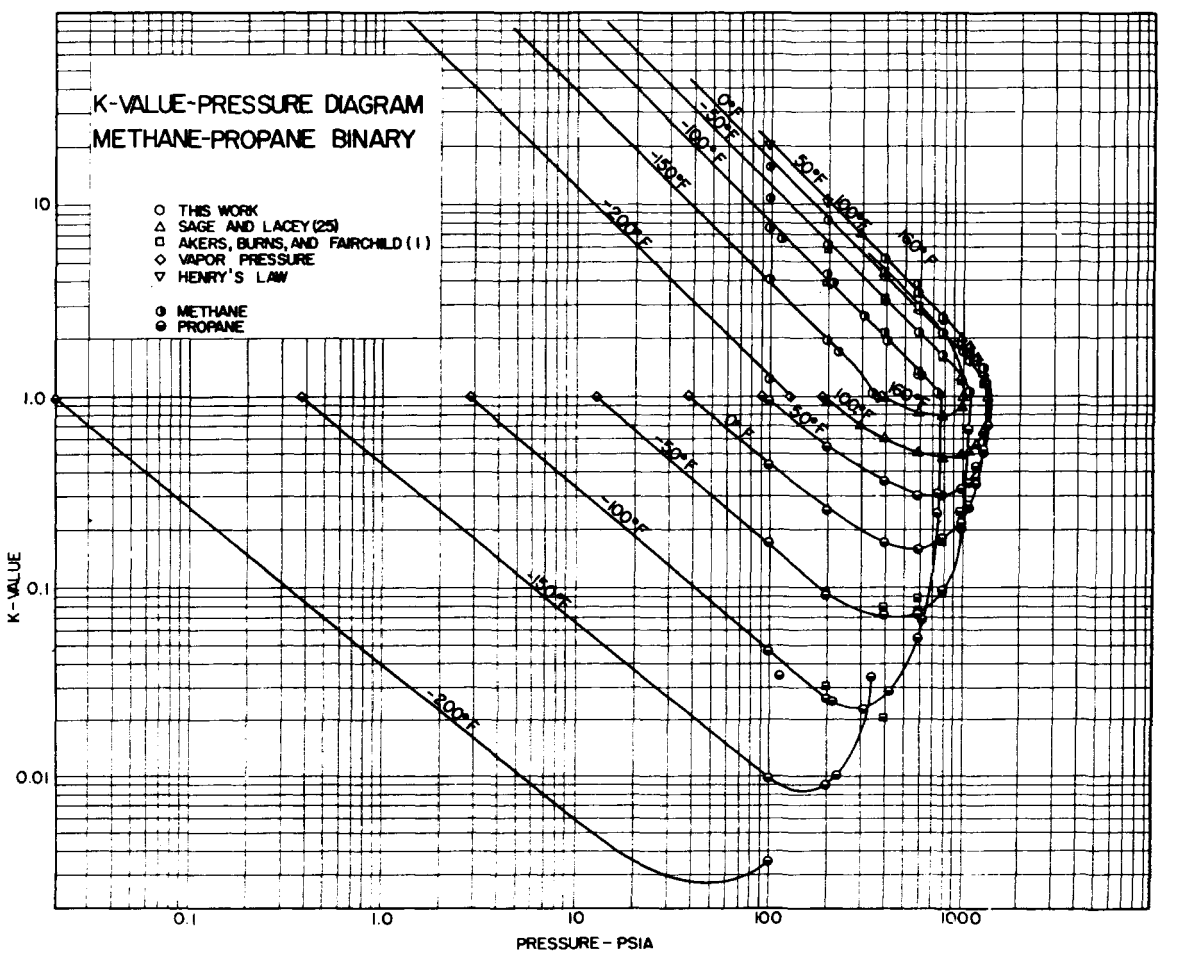

Figure 12. *K*-value–pressure diagram for methane-propane system

usually good, but greater weight was given the GLPC analyses. The infrared method was particularly valuable for approximate analyses during attempts to reach a desired composition. This type of analysis could be performed in a very few minutes, whereas a complete chromatographic analysis required about an hour.

EXPERIMENTAL RESULTS

Equilibrium measurements were made on more than 150 mixtures involving methane, ethane, and propane over a wide range of temperatures and pressures. Conditions investigated are given below:

Temperature, °F.	Pressure, P.S.I.A.
50	100, 200, 400, 600, 800, 1000, 1100, 1200
0	100, 200, 400, 600, 800, 1000, 1100, 1200, 1300
- 50	100, 200, 400, 600, 800, 1000
-100	100, 200, 400, 600
-150	100, 200
-200	100

A complete tabulation of all binary and ternary data obtained in this investigation appears in Table II.

Presentation of Binary Equilibrium Data. The results of binary equilibrium measurements from this work have been plotted in various ways. Related data from other sources have been included where applicable.

The pressure-temperature projection showing vapor pressures of methane, ethane, propane, and *n*-butane is given in Figure 7. Included are the known critical loci for the associated binary systems.

Pressure-composition diagrams for the systems methane-ethane and methane-propane from this work are shown in Figures 8 and 9.

K-value *vs.* pressure and *K*-values *vs.* temperatures are plotted in Figures 10 to 13 for the same systems. In low pressure regions where either the Henry-Dalton or the Raoult-Dalton relationships hold, the log *K* *vs.* log *P* curves become 45 degree lines. These rules may be applied in the extension of high pressure data to lower pres-

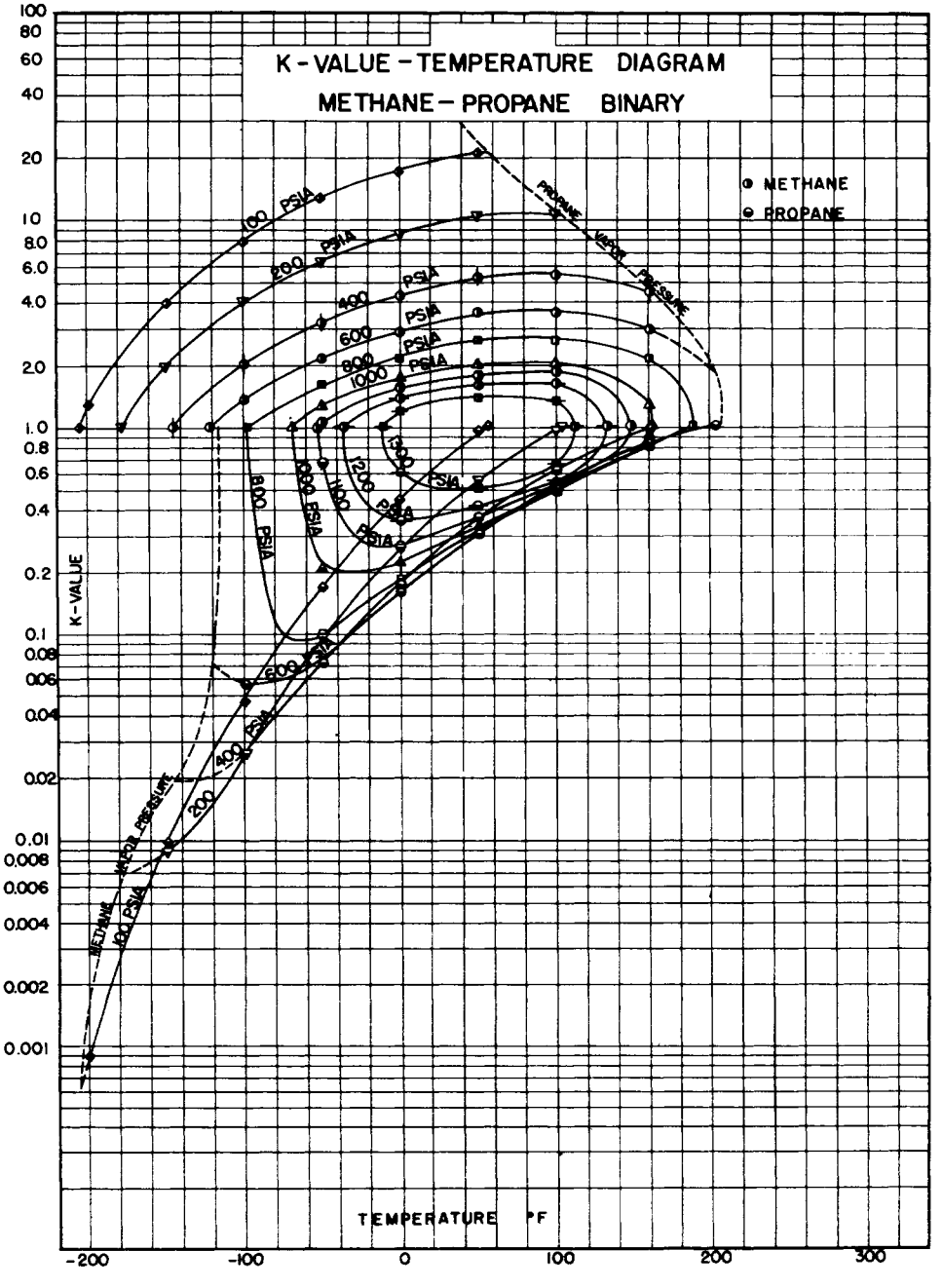

Figure 13. *K*-value-temperature diagram for methane-propane system

sures. In particular, the Raoult-Dalton relationship is useful, since the vapor pressure of the less volatile component provides an anchor point for the K-value of the component at low pressures.

The actual experimental data have been plotted on the K-P diagrams (Figure 10 and 12), whereas smoothed values, taken from these curves appear on the K-T graphs (Figures 11 and 13). The dotted extensions of the curves for pressures below the critical are estimations and the accuracy should be interpreted accordingly. They terminate when the value of the boiling point at the particular value of pressure is reached.

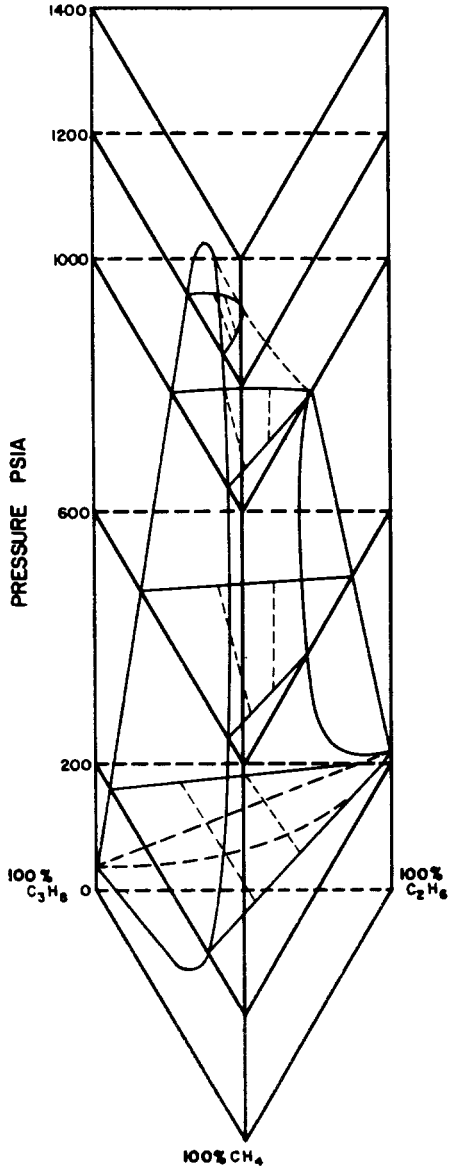

Figure 14. Pressure-composition diagram for ternary system at 0° F.

Presentation of Ternary Equilibrium Data. For a ternary system, complete representation of two-phase equilibrium requires the definition of three independent variables. Thus, at a given temperature, ternary equilibria may be represented in three dimensions. Figure 14 shows a pressure-composition diagram for the ternary mixture at 0°F. The faces of the prism are recognized as being the binary P-X plots. They bound the three-dimensional figure repre-

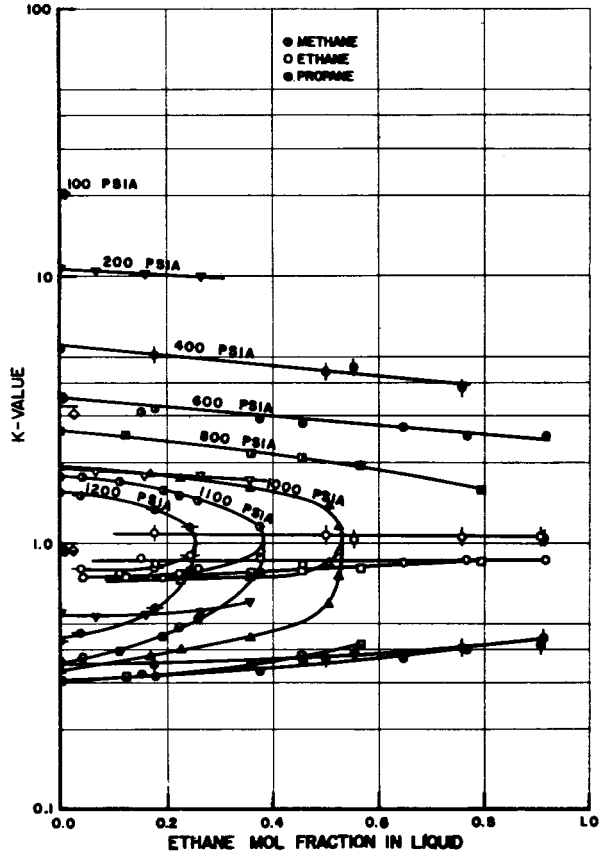

Figure 15. K-value-composition diagram for ternary system at 50° F.

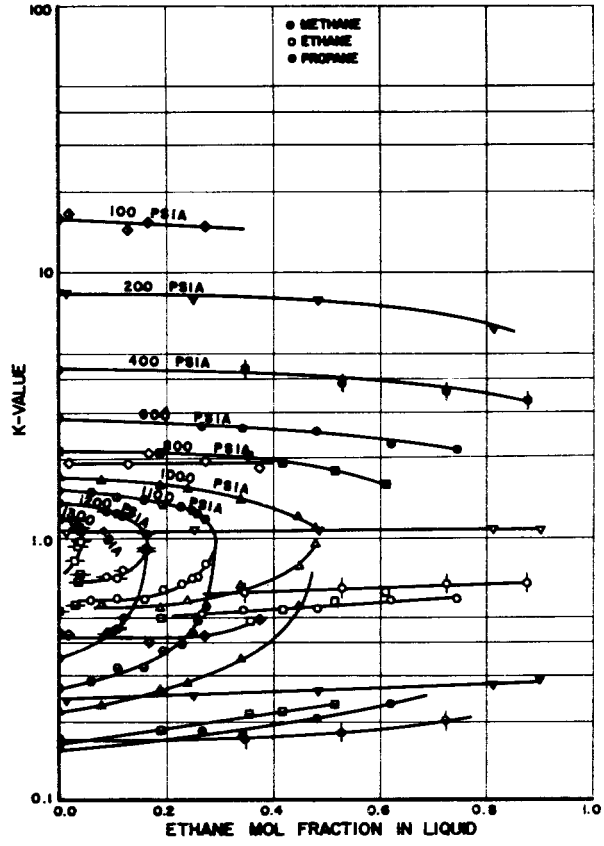

Figure 16. K-value-composition diagram for ternary system at 0° F.

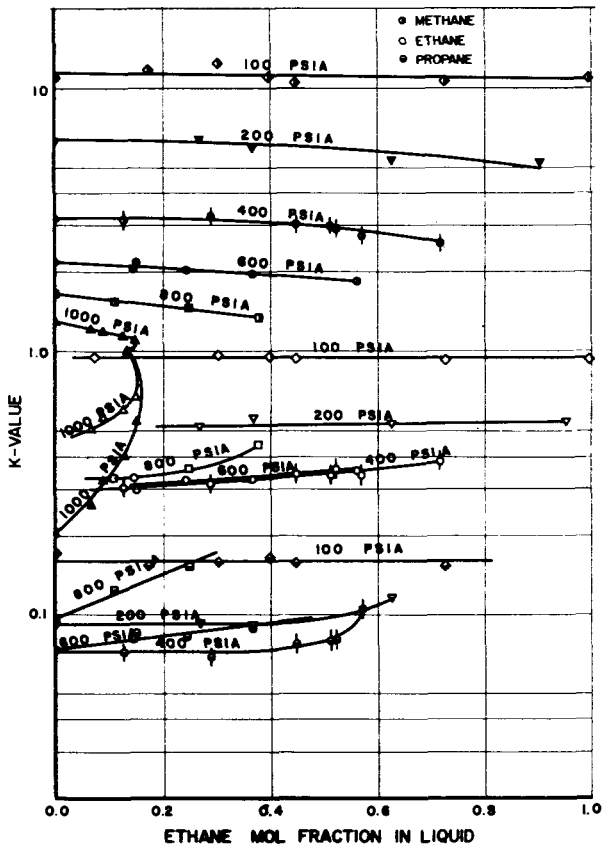

Figure 17. *K*-value-composition diagram for ternary system at −50° F.

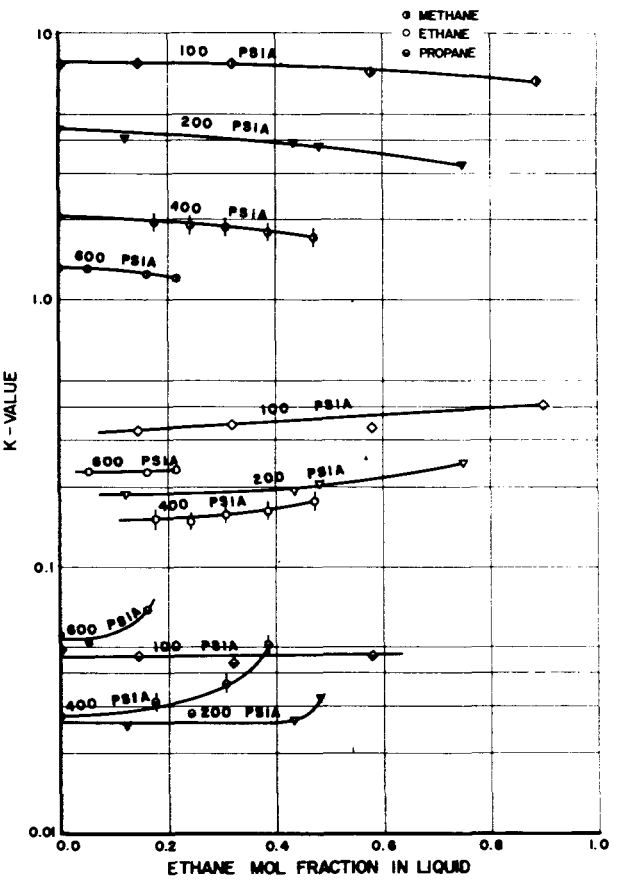

Figure 18. *K*-value-composition diagram for ternary system at −100° F.

senting the ternary system. Several constant pressure sections are shown, intersecting the equilibrium surfaces along the solid lines, with example tie lines being dotted. Such diagrams can be constructed for various temperatures, representing the entire vapor-liquid region. While this type of representation is important qualitatively, its quantitative value is limited.

To represent the experimentally determined *K*-values, some composition variable must be included with temperature and pressure. It is customary to use the composition of a component in one of the equilibrium phases or some function of phase composition. In this work, the ethane concentration in the liquid was selected because its degree of variation was generally the greatest. The experimental data are plotted as log *K* *vs.* ethane concentration in the liquid with parameters of constant pressure for each temperature. The graphs appear as Figures 15 to 20.

Because of extremely low concentrations of methane in the liquid phase at 50°F. for the 100 and 200 p.s.i. runs, the analytical accuracy is doubtful. A method of predicting the data in this region was therefore selected. The binary *K*-values were obtained by assuming Henry's law and extending the curves as 45° lines into the low pressure region, as was previously discussed. Although not strictly applicable to ternaries, the method was used in a modified form. A hypothetical binary was assumed by taking *K*-values of propane from the propane *K* *vs.* ethane concentration plots at constant concentrations of ethane in the liquid. The *K*-*P* curves thus obtained were extended as before into the low pressure region to get *K*-values.

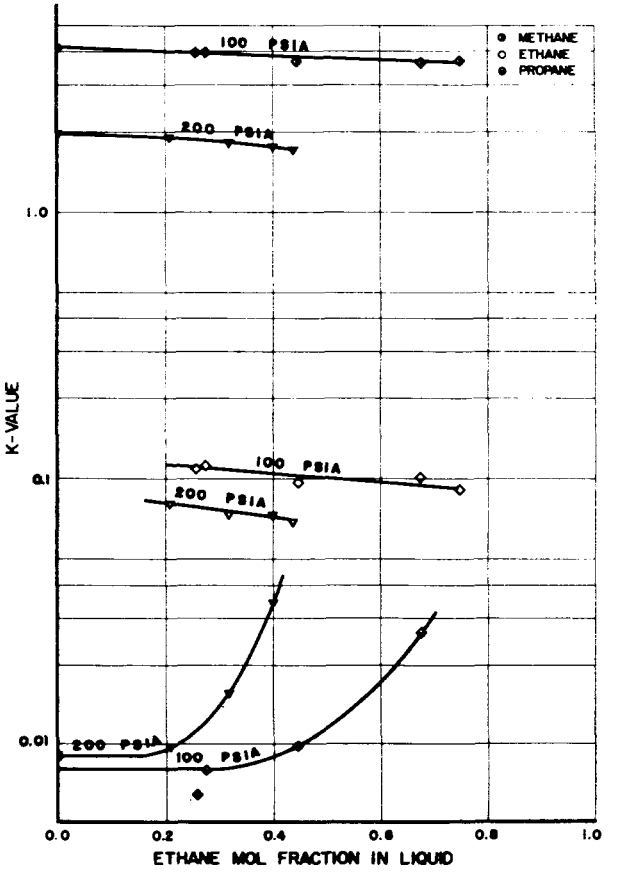

Figure 19. *K*-value-composition diagram for ternary system at −150° F.

Analytical difficulties were also encountered at very low temperatures where the concentration of the heavier components in the vapor is low. Unfortunately, Raoult's law cannot be applied to smooth the K-values of ethane and propane at −200°F. because their concentration in the liquid is not high enough to consider them as solvents. The −200°F. curve for propane K-value in the K-P diagram of the methane-propane binary (Figure 12) was used as a basis. An experimental K-value for propane of 0.0035 was assumed correct with relation to the higher isotherms. The measured propane concentration in the vapor phase was about 0.07 mole %. Previous data (Table II) have indicated that the vapor phase becomes consistently leaner in propane as ethane is increased in the liquid. As a conservative move, the propane concentration in the vapor

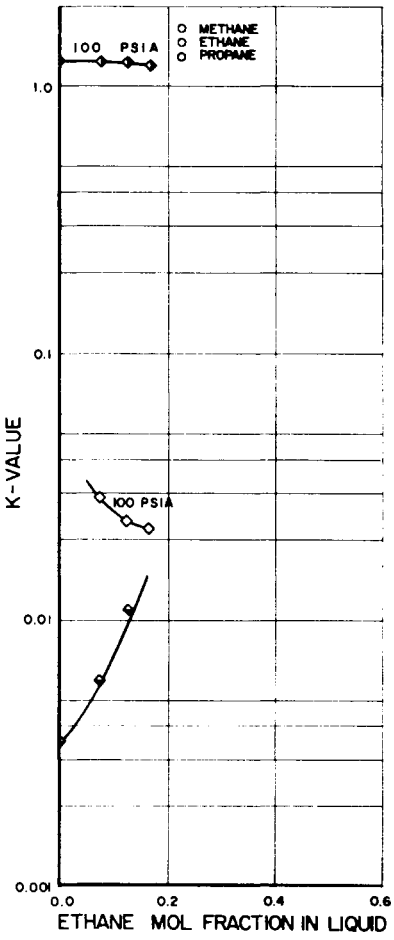

Figure 20. K-value-composition diagram for ternary system at −200° F.

was assumed constant at 0.07 % as the liquid changed, yielding the curve in Figure 20. This should represent the *maximum* K-value curve for propane at −200°F. and 100 p.s.i.a.

GENERAL COMMENTS

No retrograde condensation was observed in the external visual cell during the experimental operations. Close watch was kept, especially at high pressure conditions where the propane concentration in the vapor became large.

Critical opalescence occurred in the equilibrium cell during measurements near the critical points of the various mixtures. A rust-brown color was observed with the transmitted fluorescent light. Reflected light gave only a gray-white color. The color effect was estimated as occurring in a region within 10 p.s.i. of the critical. It was more easily obtained by approaching the critical from the high pressure side.

This phenomenon of critical opalescence has been previously investigated, from an experimental and theoretical standpoint (*4, 8, 17, 19, 30, 32, 33, 35*). It is apparently due to microscopic density fluctuations in the form of molecular clusters.

The data presented here have been used as a basis for study of the use of the Benedict-Webb-Rubin equation of state (*2*) for the estimation of low temperature phase equilibria data (*22*). The data are presented in correlative form using DePriester type plots (*22*).

ACKNOWLEDGMENT

P. D. Harvey is credited for his earlier efforts in constructing and testing the experimental equipment. The research was carried out under generous fellowship grants from the American Oil Co., Standolind Oil and Gas Co., and Dow Chemical Co. Phillips Petroleum Co. and the Tennessee Gas Transmission Co. supplied the pure hydrocarbons.

LITERATURE CITED

(1) Akers, W. W., Burns, J. F., Fairchild, W. R., *Ind. Eng. Chem.* **46**, 2531 (1954).
(2) Benedict, M., Webb, G. B., Rubin, L. C., *J. Chem. Phys.* **8**, 334 (1940).
(3) Bloomer, O. T., Gami, D. C., Parent, J. D., Inst. Gas Technol., Research Bull. 22 (July 1953).
(4) Booth, H. S., Wilson, K. S., *J. Am. Chem. Soc.* **57**, 2280 (1935).
(5) Bradford, B. W., Harvery, D., Chalkley, *J. Inst. Petrol.* **41**, 375 (1955).
(6) Buckley, S. E., Lightfoot, J. H., *Petroleum Trans., AIME* **142**, 232 (1941).
(7) DePriester, C. L., *Chem. Eng. Progr. Symposium Ser.* **49** (7), 1 (1953).
(8) Donnan, F. G., *Brit. Assoc. Advance Sci. Rept.*, 1904, 504.
(9) Guter, M., Newitt, D. M., Ruhemann, M., *Proc. Roy. Soc. (London)* **176A**, 140 (1940).
(10) Harvey, P. D., M. S. thesis, Rice Institute, Houston, Tex., 1953.
(11) James, A. T., *Chem. & Process Eng.* **36**, 95 (1955).
(12) James, D. H., Phillips, C. S. G., *J. Chem. Soc.* **1953**, 1600.
(13) Kharakhorin, F. F., *J. Tech. Phys. (U.S.S.R.)* **11**, 1133 (1941).
(14) Levitskaya, E. P., *Ibid.*, **11**, 197 (1941).
(15) McCurdy, J. L., Katz, D. L., *Ind. Eng. Chem.* **36**, 675 (1944).
(16) McKay, R. A., Reamer, H. H., Sage, B. H., *Ibid.*, **43**, 2112 (1951).
(17) Mondaine-Monval, P., Quiquerez, J., *Bull. soc. chim.* **12**, 380 (1945).
(18) Nederbragt, G. W., *Ind. Eng. Chem.* **30**, 587 (1938).
(19) Olds, R. H., Sage, B. H., Lacey, W. N., *Ibid.*, **34**, 1008 (1942).
(20) Patton, H. W., Lewis, J. S., Kaye, W. L., *Anal. Chem.* **27**, 170 (1955).
(21) Phillips, C. S. G., *Discussions Faraday Soc.* **7**, 241 (1949).
(22) Price, A. R., Ph.D. thesis, Rice Institute, 1957.
(23) Price, A. R., Leland, T. W., Kobayashi, R., Evaluation of Benedict-Webb-Rubin Equation for Prediction of Phase Equilibrium of Light Hydrocarbon Mixtures at Low Temperatures, *Chem. Eng. Progr. Symposium Ser.* **21**, 54 (1958).
(24) Ray, M. H., *J. Appl. Chem. (London)* **4** (21), 82 (1954).
(25) Ruheman, M., *Proc. Roy. Soc. (London)* **171 A** (1939).
(26) Ruheman, M., "Separation of Gases," 2nd ed., Oxford University Press, 1949.
(27) Sage, B. H., Lacey, W. N., Oxford, England, Schassfma, J. G., *Ind. Eng. Chem.* **26**, 214 (1934).
(28) Shearer, L. T., Kobayashi, R., Rice Institute, Houston, Tex., unpublished data, August 1956.
(29) Silberberg, I. H., Kuo, P. K., McKetta, J. J., *Petrol. Engr.* **24** (5), C5–10 (May 1952).
(30) Smoluchowski, M. S., *Phil. Mag. (VI)* **23**, 165 (1912).
(31) Stutzman, L. F., Brown, G. G., *Chem. Eng. Progr.* **45**, 139 (1949).
(32) Travers, F. R. S., Usher, F. L., *Proc. Roy. Soc. (London)* **78A**, 247 (1906).
(33) Villard, P., *Ann. chim. et phys.* (Ser. 7), 387 (1897).
(34) Volova, L. M., *J. Phys. Chem. (U.S.S.R.)* **14**, 268 (1940).
(35) Zernike, F., *Arch. neerl. sci.* **IIIA**, **4**, 74 (1917).

Received for review March 16, 1957. Accepted January 24, 1958.